



Shape diagrams for 2D compact sets - Part III: convexity discrimination for analytic and discretized simply connected sets.

Séverine Rivollier, Johan Debayle, Jean-Charles Pinoli

► To cite this version:

Séverine Rivollier, Johan Debayle, Jean-Charles Pinoli. Shape diagrams for 2D compact sets - Part III: convexity discrimination for analytic and discretized simply connected sets.. Australian Journal of Mathematical Analysis and Applications, 2010, 7 (2), Article 5, pp. 1-18. hal-00550951

HAL Id: hal-00550951

<https://hal.science/hal-00550951>

Submitted on 18 Jan 2011

HAL is a multi-disciplinary open access archive for the deposit and dissemination of scientific research documents, whether they are published or not. The documents may come from teaching and research institutions in France or abroad, or from public or private research centers.

L'archive ouverte pluridisciplinaire **HAL**, est destinée au dépôt et à la diffusion de documents scientifiques de niveau recherche, publiés ou non, émanant des établissements d'enseignement et de recherche français ou étrangers, des laboratoires publics ou privés.

SHAPE DIAGRAMS FOR 2D COMPACT SETS - PART III: CONVEXITY DISCRIMINATION FOR ANALYTIC AND DISCRETIZED SIMPLY CONNECTED SETS

S. RIVOLLIER, J. DEBAYLE AND J.-C. PINOLI

ABSTRACT. Shape diagrams are representations in the Euclidean plane introduced to study 3-dimensional and 2-dimensional compact convex sets. However, they can also be applied to more general compact sets than compact convex sets. A compact set is represented by a point within a shape diagram whose coordinates are morphometrical functionals defined as normalized ratios of geometrical functionals. Classically, the geometrical functionals are the area, the perimeter, the radii of the inscribed and circumscribed circles, and the minimum and maximum Feret diameters. They allow twenty-two shape diagrams to be built. Starting from these six classical geometrical functionals, a detailed comparative study has been performed in order to analyze the representation relevance and discrimination power of these twenty-two shape diagrams. The two first parts of this study are published in previous papers [8, 9]. They focus on analytic compact convex sets and analytic simply connected compact sets, respectively. The purpose of this paper is to present the third part, by focusing on the convexity discrimination for analytic and discretized simply connected compact sets.

1 INTRODUCTION

The Santalo's shape diagrams [10] allow to represent a 2D compact convex set by a point in the Euclidean 2D plane from six geometrical functionals: the area, the perimeter, the radii of the inscribed and circumscribed circles, and the minimum and maximum Feret diameters [4]. The axes of each shape diagram are defined from a pair of geometric inequalities relating these functionals. Sometimes, the two geometric inequalities provide a complete system: for any range of numerical values satisfying them, there exists a compact convex set with these values for the geometrical functionals (in other words, a point within the 2D Santalo shape diagram describes a 2D compact convex set). This is not valid for all the Santalo shape diagrams.

This paper deals with the study of the convexity discrimination for shape diagrams of 2D non-empty analytic and discretized simply connected compact sets. The two first parts [8, 9] of this study focus on the analytic compact convex sets and analytic simply connected compact sets, respectively. This third part presents an analysis of the convexity discrimination and extends the previous work to the discretized simply connected compact sets. The considered discretized simply connected sets are mapped onto points in these shape diagrams, and through dispersion quantification and convexity discrimination, the shape diagrams are classified according to their ability to discriminate the simply connected compact sets.

Key words and phrases. Analytic and discretized simply connected compact sets, Convexity discrimination, Geometrical and morphometrical functionals, Shape diagrams, Shape discrimination.

2 SHAPE CONVEXITY

The following study on the convexity discrimination first requires the definition of the shape convexity. A set is convex when the line segment which joins any two points in it lies totally within the set. In other terms, the shape convexity could be quantified with the probability that two points in the set lies totally within it.

Convexity parameters are commonly used in the analysis of shapes. The measurement value of the shape convexity of any set ranges between 0 and 1 (it is a probability). A convex set gives the value 1. Furthermore, the less the parameter value is high, the less the shape is convex. The convexity measurement can be computed, for instance, by the ratio A / A_C where A_C is the area of the convex hull of the set, but this is not sensitive to boundary small variations (Figure 2.1). A second convexity parameter is the ratio P_C / P where P_C is the Euclidean perimeter of the convex hull of the set.

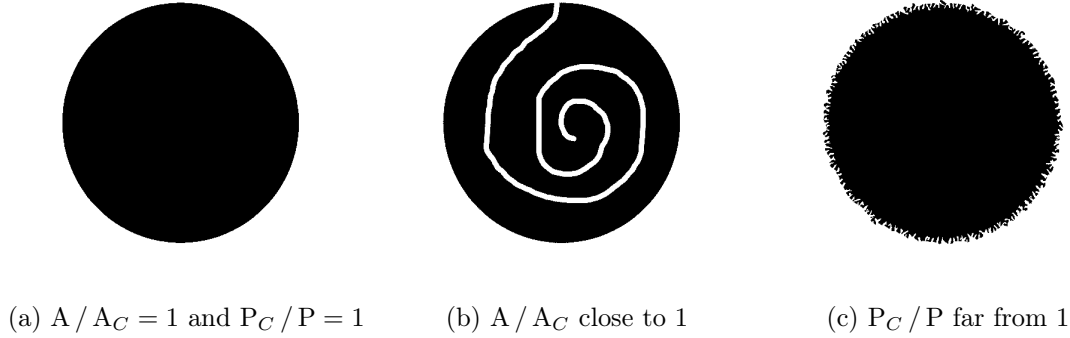


Figure 2.1: A / A_C gives result values equal to 1 for the set (a) and close to 1 for the sets (b) and (c). Nevertheless, the set (b) is far to check the convexity definition (the probability that two points in the set lies totally within it is low). P_C / P gives result values equal to 1 for the set (a) and far from 1 for the sets (b) and (c). Nevertheless, the set (c) is not very far to check the convexity definition.

Futhermore, a suitable convexity parameter is particularly required for discretized sets. For that purpose, the convexity parameter of Zunic and Rosin [12] will be used for the following study on the convexity discrimination. For all polygon S of the Euclidean 2D plane \mathbb{E}^2 , it is defined by:

$$(2.1) \quad c(S) = \min_{\alpha \in [0, 2\pi]} \frac{P_2(R(S, \alpha))}{P_1(S, \alpha)}$$

$P_1(S, \alpha)$ denotes the perimeter of the set S , rotated by the angle α with the origin as the center of rotation, in the sense of the l_1 metric ($l_1(e)$ equals the sum of the projections of the straight line segment e onto the coordinate axes). $P_2(R(S, \alpha))$ denotes the Euclidean perimeter of the minimal bounding rectangle R with edges parallel to the coordinate axes which includes the rotated set of S by the angle α .

This convexity parameter c has the following desirable properties:

- its value is always a number within $(0, 1]$
- its value is 1 if and only if the measured set is convex
- there are sets with its value arbitrarily close to 0

- it is invariant under similitude transformations
- there is a simple and fast procedure for computing it.

3 CONVEXITY DISCRIMINATION FOR ANALYTIC SIMPLY CONNECTED SETS

Observing the 2D compact set locations in the shape diagrams \mathcal{D}_k , $k \in \llbracket 1, 30 \rrbracket \setminus (\llbracket 7, 10 \rrbracket \cup \llbracket 17, 20 \rrbracket)$ for the families \mathcal{F}_1^c and \mathcal{F}_1^{sc} [8, 9] (Figures 3.1 and 3.2), some shape diagrams seem to stronger discriminate the convex shapes from the non-convex shapes than others.

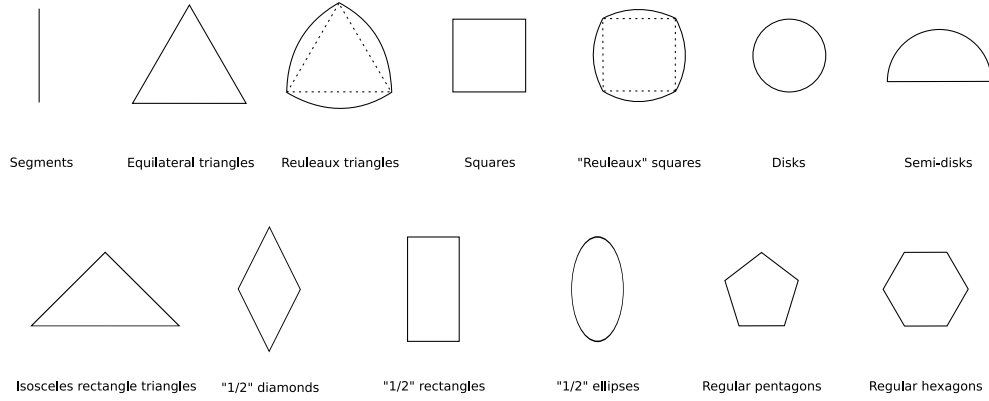


Figure 3.1: Family \mathcal{F}_1^c of 2D analytic compact convex sets [8].

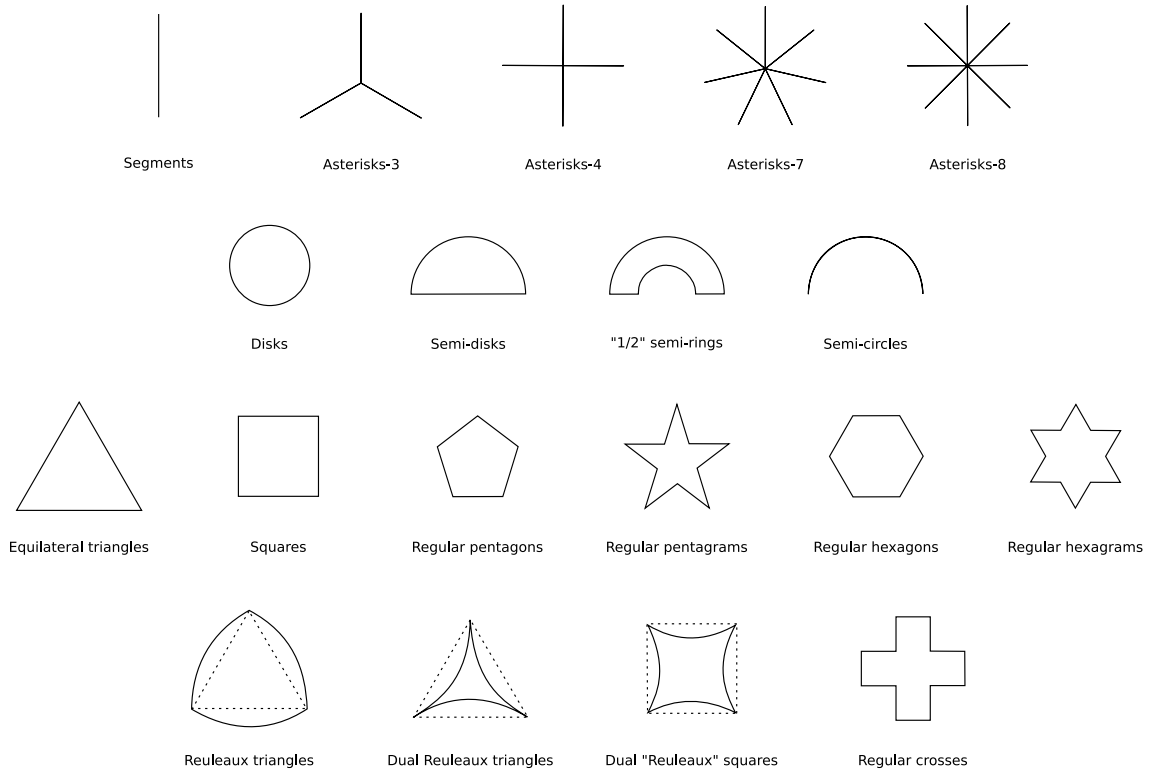


Figure 3.2: Family \mathcal{F}_1^{sc} of 2D analytic simply connected compact sets [9].

Equation 3.1 quantifies (by values ranging between 0 and 1) this convexity discrimination for each shape diagram \mathcal{D}_k , $k \in \llbracket 1, 30 \rrbracket \setminus (\llbracket 7, 10 \rrbracket \cup \llbracket 17, 20 \rrbracket)$. A high (respectively low) resulting value means a weak (respectively strong) convexity discrimination.

$$(3.1) \quad \text{Convexity_discrimination}(\mathcal{D}_k) = \frac{1}{\# \{\mathcal{F}_1^c \cup \mathcal{F}_1^{sc}\}} \left(\sum_{i=1}^{\#\mathcal{F}_1^c} |c(i) - c(\argmin \{d_E(i, j) | j \in \mathcal{F}_1^{sc}\})| + \sum_{i=1}^{\#\mathcal{F}_1^{sc}} |c(i) - c(\argmin \{d_E(i, j) | j \in \mathcal{F}_1^c\})| \right)$$

where $c(i)$ denotes the convexity value of the shape indexed by i in Figure 5.1, and d_E is the Euclidean distance.

Figure 3.3 shows the results of this quantification for every shape diagrams \mathcal{D}_k , $k \in \llbracket 1, 30 \rrbracket \setminus (\llbracket 7, 10 \rrbracket \cup \llbracket 17, 20 \rrbracket)$. The stronger convexity discrimination appears in the shape diagrams \mathcal{D}_{24} , \mathcal{D}_{26} , \mathcal{D}_{27} , and \mathcal{D}_{29} , that is in agreement with the visual interpretation [9], and the weaker discrimination appears for the shape diagrams \mathcal{D}_4 and \mathcal{D}_{14} .

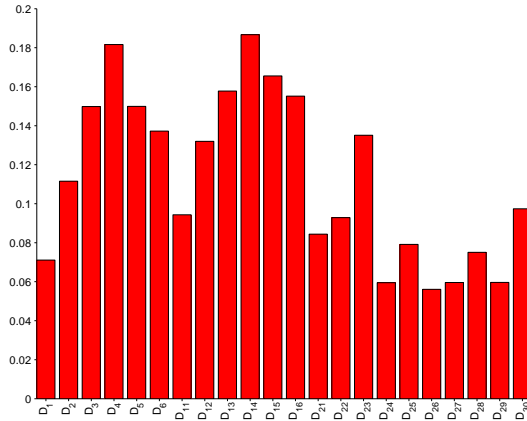


Figure 3.3: Convexity discrimination for the families \mathcal{F}_1^c and \mathcal{F}_1^{sc} .

These results have to be confirmed with more general sets. This is not easy to conclude with the restriction to analytic sets. For this reason, this study is extended to the discrete case.

4 SHAPE FUNCTIONALS FOR A DISCRETIZED SIMPLY CONNECTED SET

In this paper, the non-empty discretized simply connected compact sets in the discrete Euclidean 2-space \mathbb{E}_d^2 are considered. They are represented by points. The inter-point distance is the step discretization. The discretization is fine enough to preserve the simple connectivity [5]. For the characterization of these sets, six geometrical functionals are used allowing to define morphometrical functionals from geometric inequalities.

4.1 Geometrical functionals For a discretized simply connected compact set in \mathbb{E}_d^2 , let A , P , r , R , ω , d , denote the estimations of its area, its perimeter, the radii of its inscribed and circumscribed circles, its minimum and maximum Feret diameters [4], respectively. Figure 4.1 illustrates these geometrical functionals for a discretized simply connected compact set represented in a point lattice [5]. For all non-empty discretized simply connected compact sets, these geometrical functionals are greater or equal than zero.

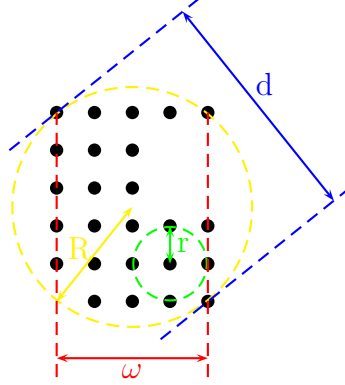


Figure 4.1: Geometrical functionals of a discretized simply connected compact set: radii of inscribed (r) and circumscribed (R) circles, minimum (ω) and maximum (d) Feret diameters. The area A is given by the point number, and the perimeter is estimated thanks to the Cauchy-Crofton-Poincaré formula [2, 3, 6].

4.2 Geometric inequalities and morphometrical functionals Geometric inequalities and morphometrical functionals for analytic simply connected compact sets are referenced in [9]. There exists special cases where a discretized set has geometrical functional values that do not verify a geometric inequality, due to the estimation error (because of the discretization). This means that this set is a discretization of an extremal set for the associated geometric inequality. Consequently, for practical reasons, the morphometrical functional value greater than one is reduced to one. Thus, the twenty-two shape diagrams referenced in [9] can be used for discretized simply connected compact sets.

5 SHAPE DIAGRAMS FOR A BASIS OF VARIOUS DISCRETIZED SIMPLY CONNECTED COMPACT SETS

5.1 Shape diagrams Figure 5.1 illustrates seventy-eight discretized patterns constituting the family \mathcal{F}_1^{dsc} . It is assumed that the discretization process is fine enough such that each discretized pattern is a discretized simply connected compact set on the points lattice [5]. Thus, the morphometrical functionals are computed and located in each shape diagram.

The discretized patterns are numerated from one to seventy-eight. The pattern number are mapped to its proper point in each shape diagram. Figure 5.2 illustrates several of these twenty-two shape diagrams, chosen according to the synthesized results of [9]. The color of the number is related to the convexity parameter value c of the associated set (dark red for a high c value, dark blue for a low c value). Moreover, the black curves indicate the convex domain boundary, if it is known [8].

Sometimes, a dark red number appears slightly outside this domain. This is mainly due to the estimation error (discretization) of the geometrical functionals. This convexity range will enable to analyze the convexity discrimination within shape diagrams.

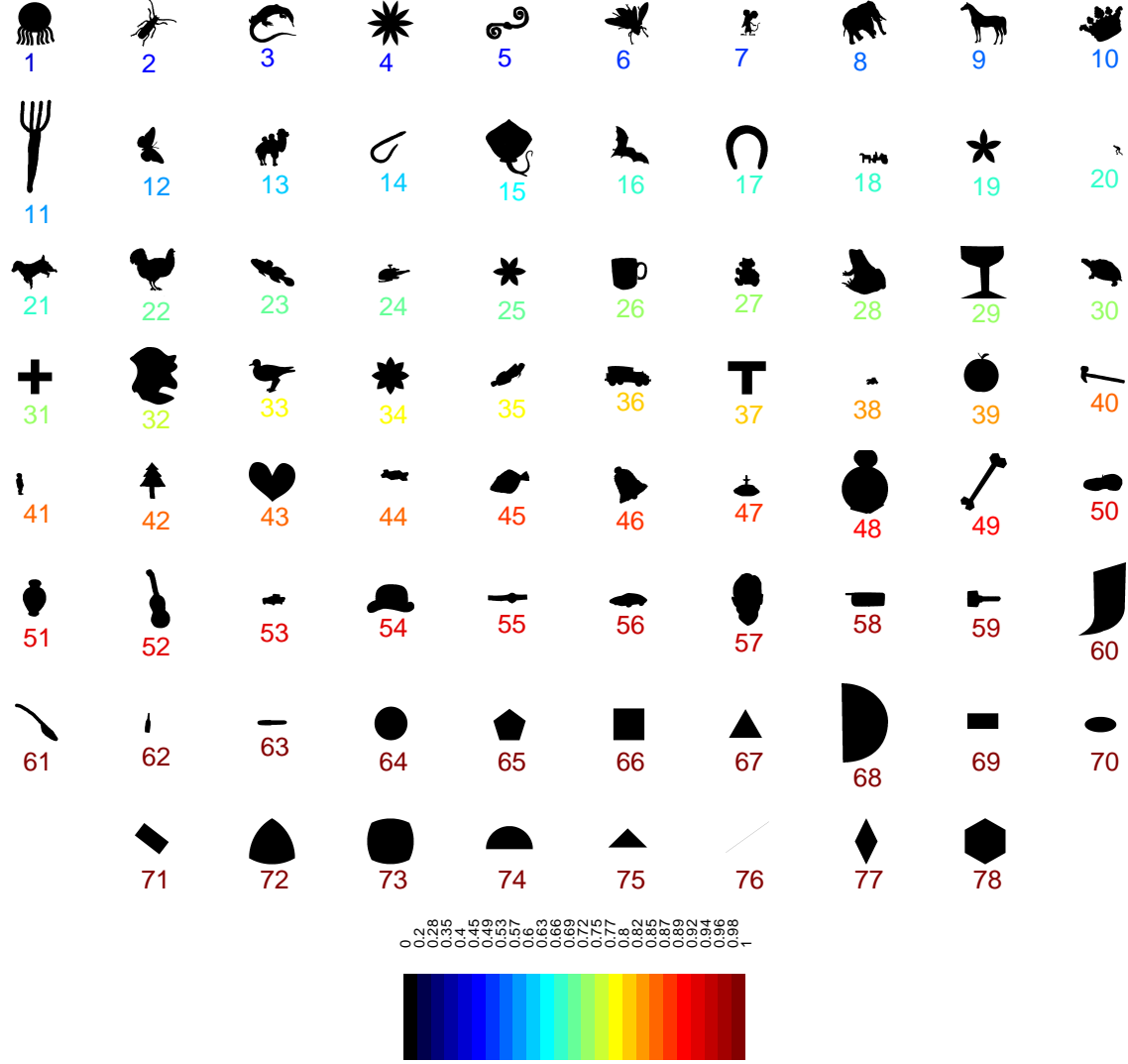


Figure 5.1: Family \mathcal{F}_1^{dsc} of seventy-eight 2D discretized simply connected compact sets (discretized patterns). The color of each pattern number is related to the convexity parameter value using non-linear color-tones.

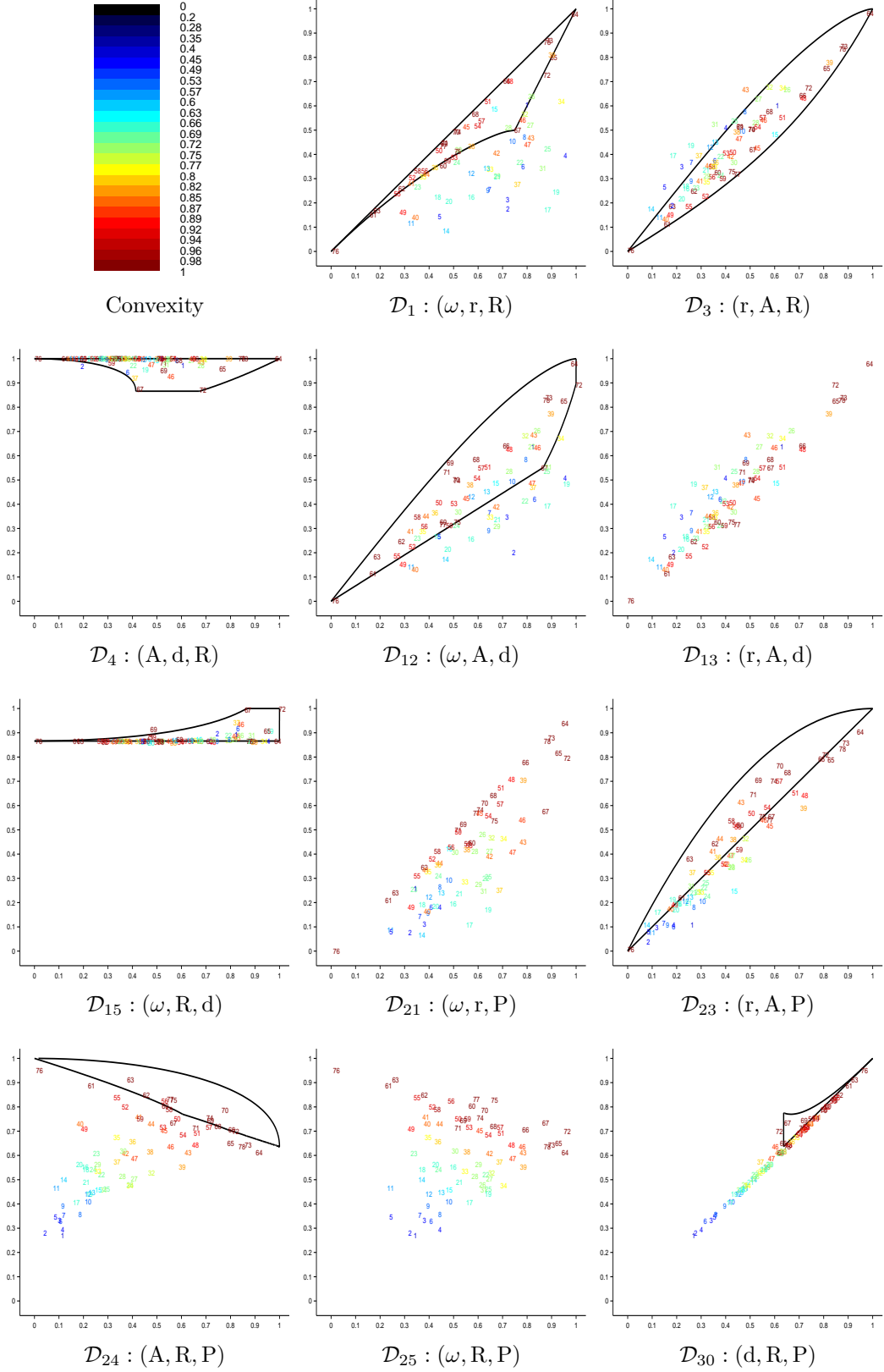


Figure 5.2: Family \mathcal{F}_1^{dsc} of discretized simply connected compact sets mapped into eleven shape diagrams (chosen according to the results synthesized in [9]).

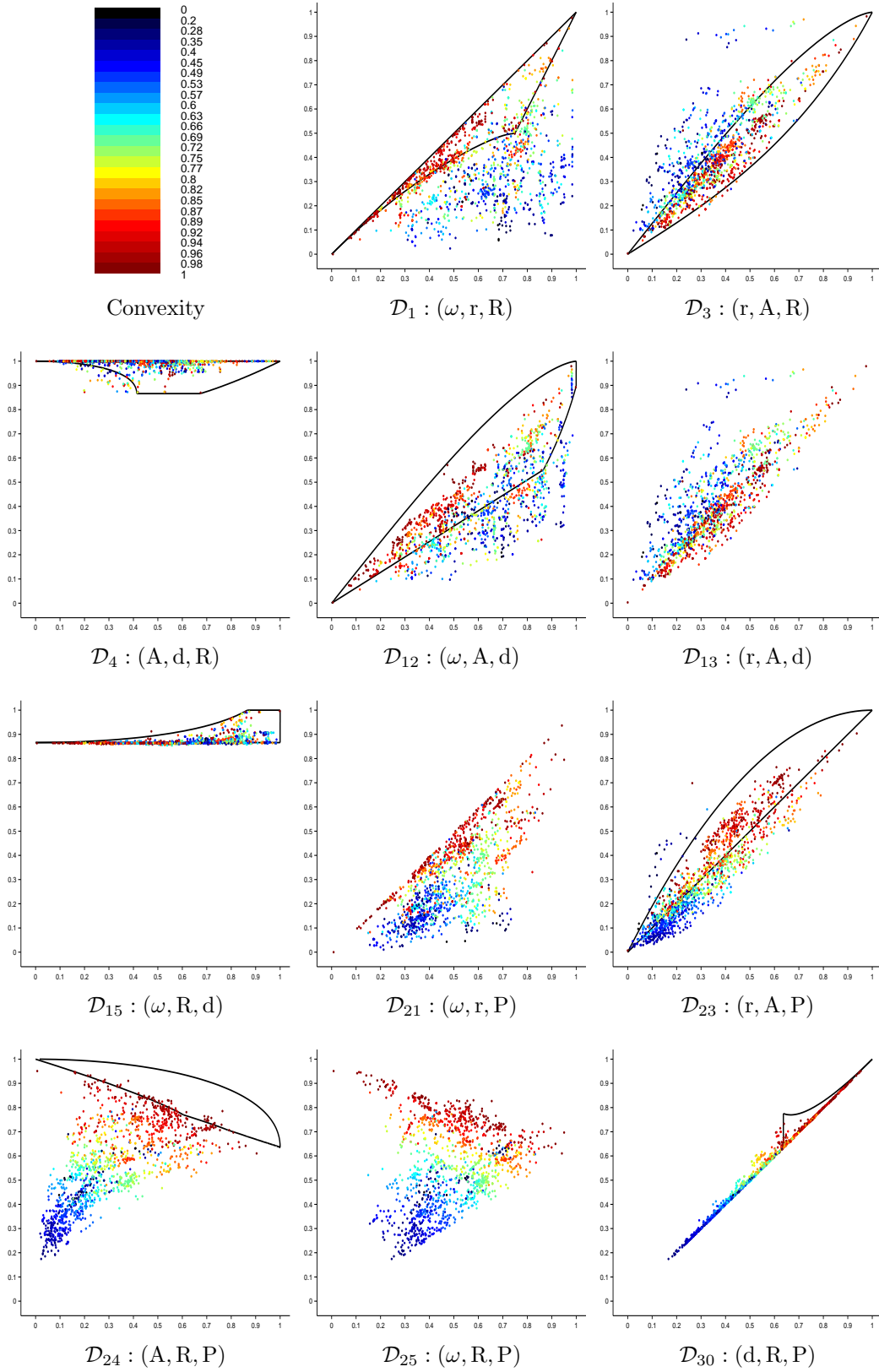


Figure 5.3: Family $\mathcal{F}_2^{\text{dsc}}$ of discretized simply connected compact sets mapped into eleven shape diagrams (chosen according to the results synthesized in [9]).

5.2 Dispersion quantification and convexity discrimination A wider family \mathcal{F}_2^{dsc} of 1370 discretized patterns is considered (Kimia database [11], not illustrated here). These are twenty deformations of each of the sixty-eight first sets of the family \mathcal{F}_1^{dsc} , plus the ten last sets of \mathcal{F}_1^{dsc} ; section 6 shows two examples of these deformations). For each discretized pattern representing a discretized simply connected compact set, the morphometrical functionals are computed and located by a point in each shape diagram (Figure 5.3). The point color is associated to the convexity parameter value c , and the convex domain boundary, if it is known, is illustrated with black lines.

5.2.1 Dispersion quantification For each shape diagram, the dispersion of the locations of the 2D discretized simply connected compact sets of the family \mathcal{F}_2^{dsc} is studied.

The spatial distribution of discretized simply connected compact sets locations in each shape diagram is characterized and quantified from algorithmic geometry using Delaunay's graph (DG) and minimum spanning tree (MST) [1]. Some useful information about the disorder and the neighborhood relationships between sets can be deduced. From each geometrical model, it is possible to compute two values from the edge lengths, denoted μ (average) and σ (standard deviation) for DG or MST. The simple reading of the coordinates in the (μ, σ) -plane enables to determine the type of spatial distribution of the discretized simply connected compact set (regular, random, cluster, ...) [7]. The decrease of μ and the increase of σ characterize the shift from a regular distribution toward random and cluster distributions.

Figure 5.4 represents both values of parameters of the twenty-two shape diagrams for each model, DG and MST.

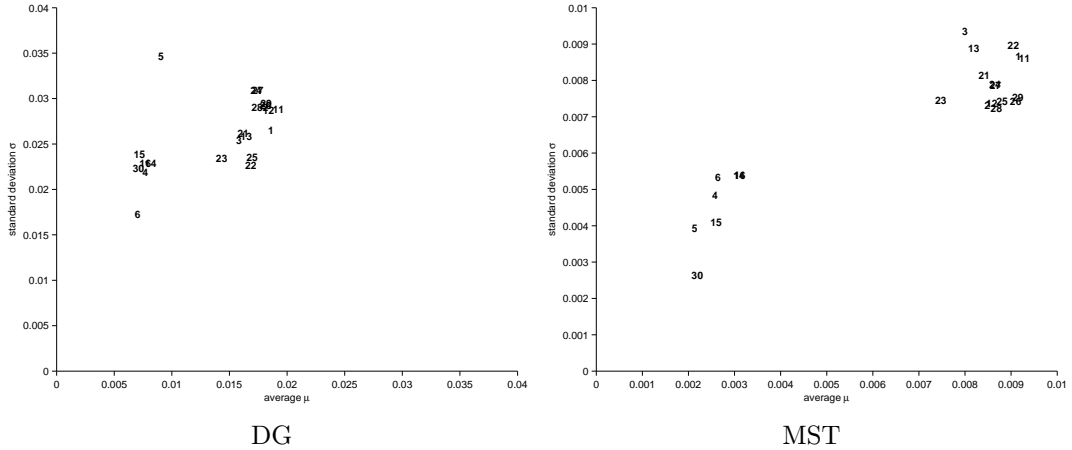


Figure 5.4: Two dispersion quantifications for all shape diagrams applied on the family \mathcal{F}_2^{dsc} . For each representation (according to the models DG and MST, respectively), indices $k \in \llbracket 1, 30 \rrbracket \setminus (\llbracket 7, 10 \rrbracket \cup \llbracket 17, 20 \rrbracket)$ of the shape diagrams \mathcal{D}_k is located according to its μ and σ values.

As in [9], the DG model allows to divide the shape diagrams into two groups, mainly according to the average μ value: the shape diagrams \mathcal{D}_4 , \mathcal{D}_5 , \mathcal{D}_6 , \mathcal{D}_{14} , \mathcal{D}_{15} , \mathcal{D}_{16} and \mathcal{D}_{30} have a weak average μ , thus the discretized simply connected compact sets are located within a small domain in $[0, 1]^2$. In [9], the MST model confirmed

this tendency for the average. Figure 5.4 shows also a distribution of these two groups according to the standard deviation σ . Note that the constitution of each of the two groups is the same as in [9].

5.2.2 Convexity discrimination Observing the colors dispersion in the shape diagrams of Figure 5.3, some shape diagrams seem to stronger discriminate the convex shapes from the non-convex shapes than others. This stronger discrimination is visually highlighted by a color gradient, from dark red to dark blue. Within a shape diagram, if the colors are irregularly distributed according to the color range, this means that convex sets and non-convex sets can not be discriminated.

Equation 5.1 quantifies (by values ranging between 0 and 1) this discrimination for each shape diagram \mathcal{D}_k , $k \in \llbracket 1, 30 \rrbracket \setminus (\llbracket 7, 10 \rrbracket \cup \llbracket 17, 20 \rrbracket)$. A high (resp. low) resulting value means a weak (resp. strong) convexity discrimination.

$$(5.1) \quad \text{Convexity_discrimination}(\mathcal{D}_k) =$$

$$\frac{1}{\#\mathcal{F}_2^{dsc}} \sum_{i=1}^{\#\mathcal{F}_2^{dsc}} |c(i) - c(\text{argmin} \{d_E(i, j) | j \in \mathcal{F}_2^{dsc}\})|$$

where $c(i)$ denotes the convexity value of the shape indexed by i in Figure 5.1, and d_E is the Euclidean distance.

Figure 5.5 shows the results of this quantification for every shape diagrams. The stronger convexity discrimination appears in the shape diagrams \mathcal{D}_{24} , \mathcal{D}_{25} , \mathcal{D}_{26} , \mathcal{D}_{27} , \mathcal{D}_{28} and \mathcal{D}_{29} , that is in agreement with the visual interpretation. The weaker discrimination appears for the shape diagrams \mathcal{D}_4 , \mathcal{D}_6 , \mathcal{D}_{14} and \mathcal{D}_{16} . Even if the shape diagram \mathcal{D}_{30} is not strong for the general shape discrimination [8, 9], it is not weak for the convexity discrimination. In fact, these two discriminations are independant.

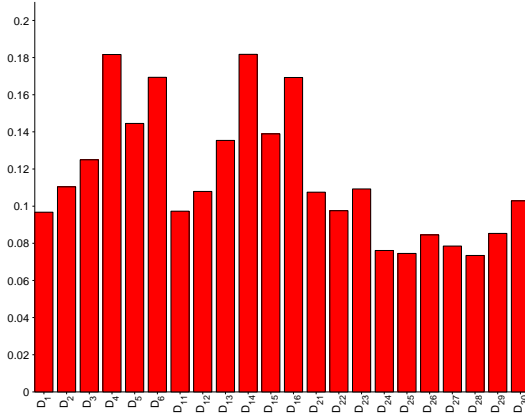


Figure 5.5: Convexity discrimination for the family \mathcal{F}_2^{dsc} .

6 SHAPE DIAGRAMS FOR SIMILAR DISCRETIZED SIMPLY CONNECTED COMPACT SETS

This section focuses on the discrimination of shapes that are visually similar enough, so that they can be considered as the same global shape. The shape diagrams \mathcal{D}_4 , \mathcal{D}_5 , \mathcal{D}_6 , \mathcal{D}_{14} , \mathcal{D}_{15} , \mathcal{D}_{16} and \mathcal{D}_{30} provide a weak shape discrimination, whatever the visual similarity of the sets. Thus, they are not considered from this section and until the end of this paper. It remains the fifteen shape diagrams \mathcal{D}_k , $k \in \llbracket 1, 29 \rrbracket \setminus (\llbracket 4, 10 \rrbracket \cup \llbracket 14, 20 \rrbracket)$.

Let be three families \mathcal{F}_3^{dsc} , \mathcal{F}_4^{dsc} and \mathcal{F}_5^{dsc} of discretized patterns representing triangles (Figure 6.1), disks (Figure 6.2) and crosses (Figure 6.3), respectively, that have undergone minor transformations, modifications, deformations. The morphometrical functionals are computed, and the patterns are located by a point in each shape diagram (Figures 6.1, 6.2 and 6.3). The color of the number is related to the convexity parameter value c , and the convex domain boundary, if it is known, is illustrated with black lines.

Figures 6.4, 6.5 and 6.6 give the dispersion quantification representation of the fifteen shape diagrams for each model, DG and MST (method described in subsubsection 5.2.1).

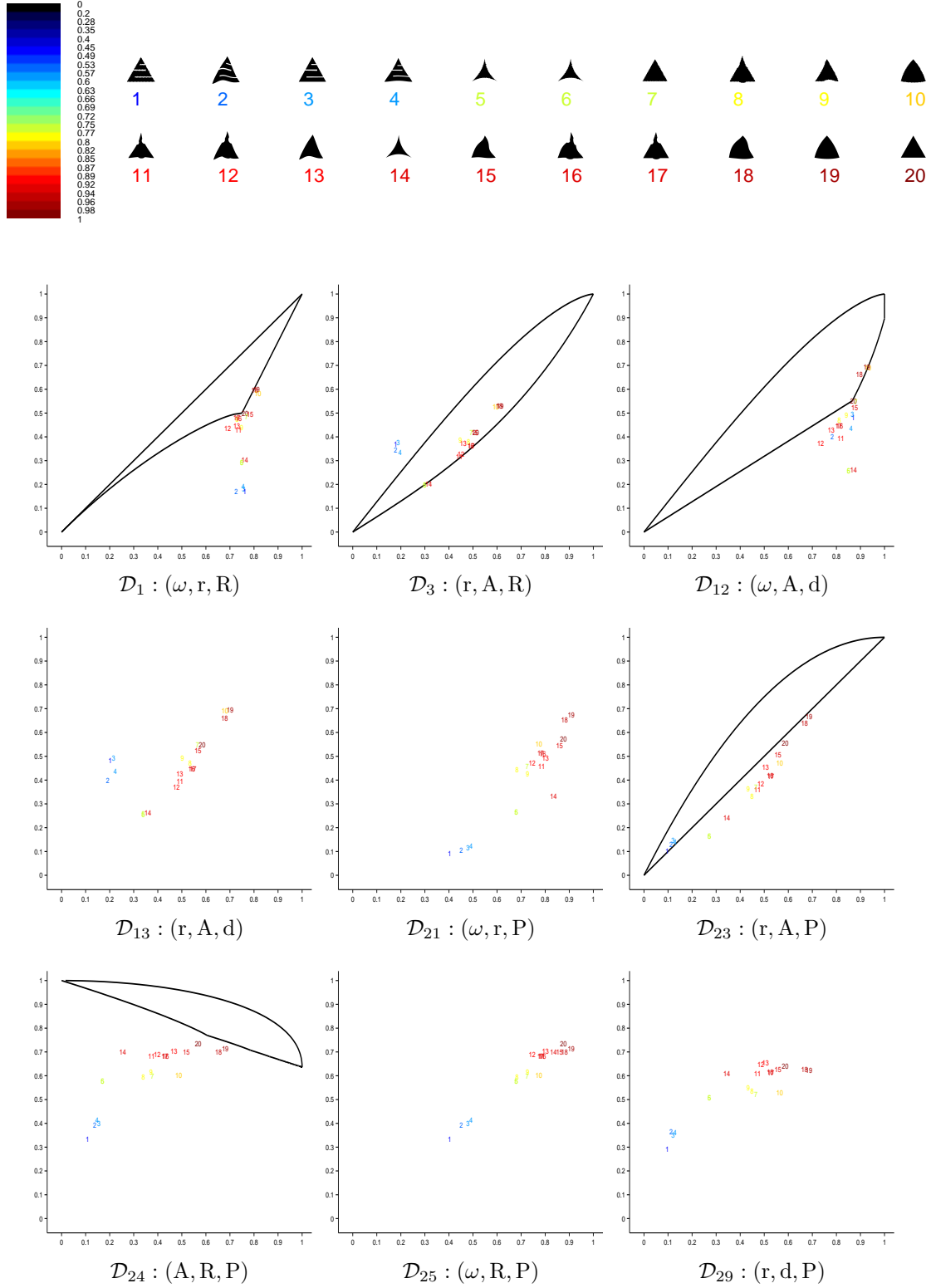


Figure 6.1: Family \mathcal{F}_3^{disc} of twenty 2D discretized simply connected compact sets with 'triangle' shape, mapped into nine shape diagrams (chosen according to the results synthetized in [9]). The color of the number is related to the convexity parameter value.

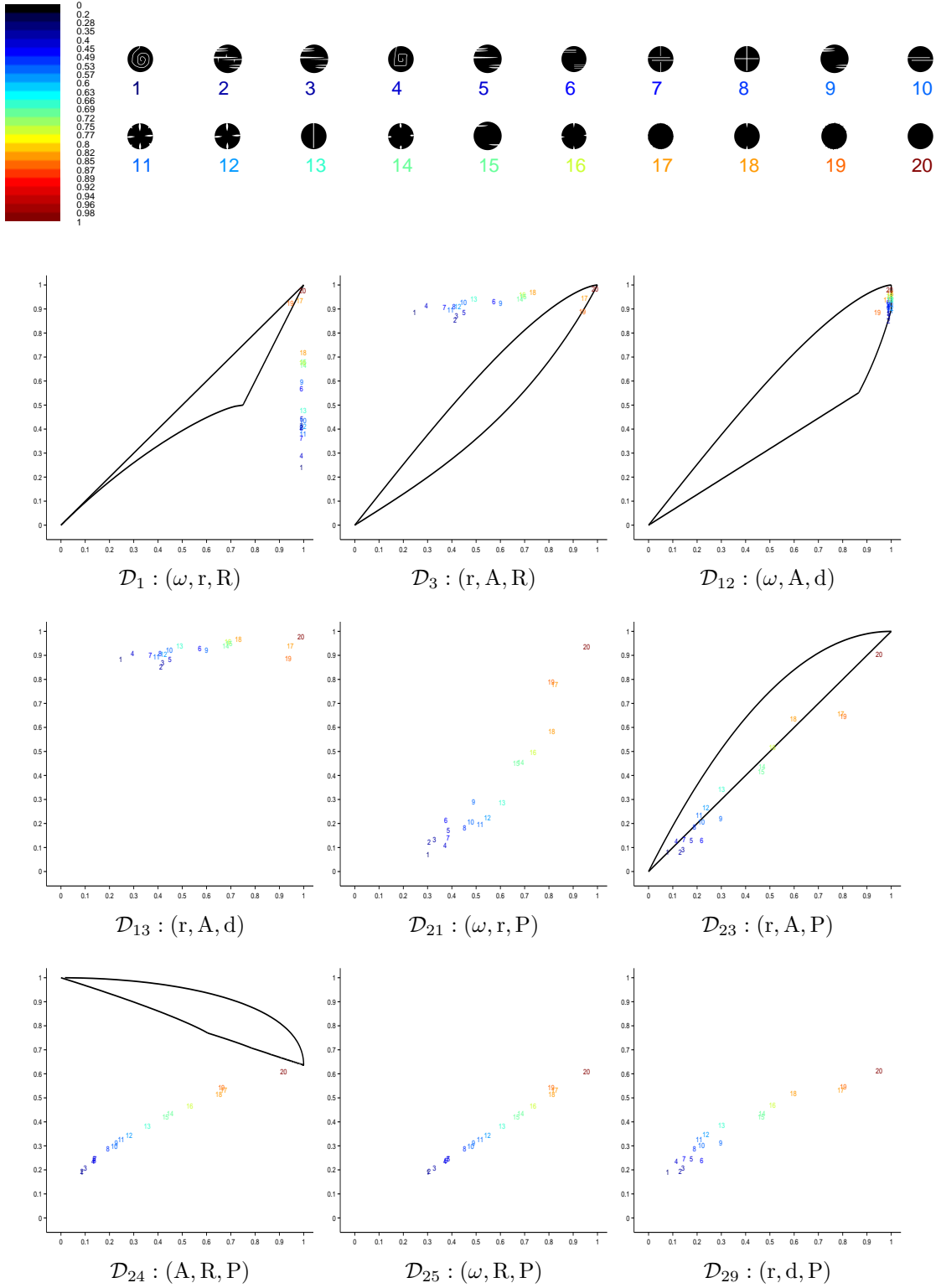


Figure 6.2: Family \mathcal{F}_4^{dsc} of twenty 2D discretized simply connected compact sets with 'disk' shape, mapped into nine shape diagrams (chosen according to the results synthesized in [9]). The color of the number is related to the convexity parameter value.

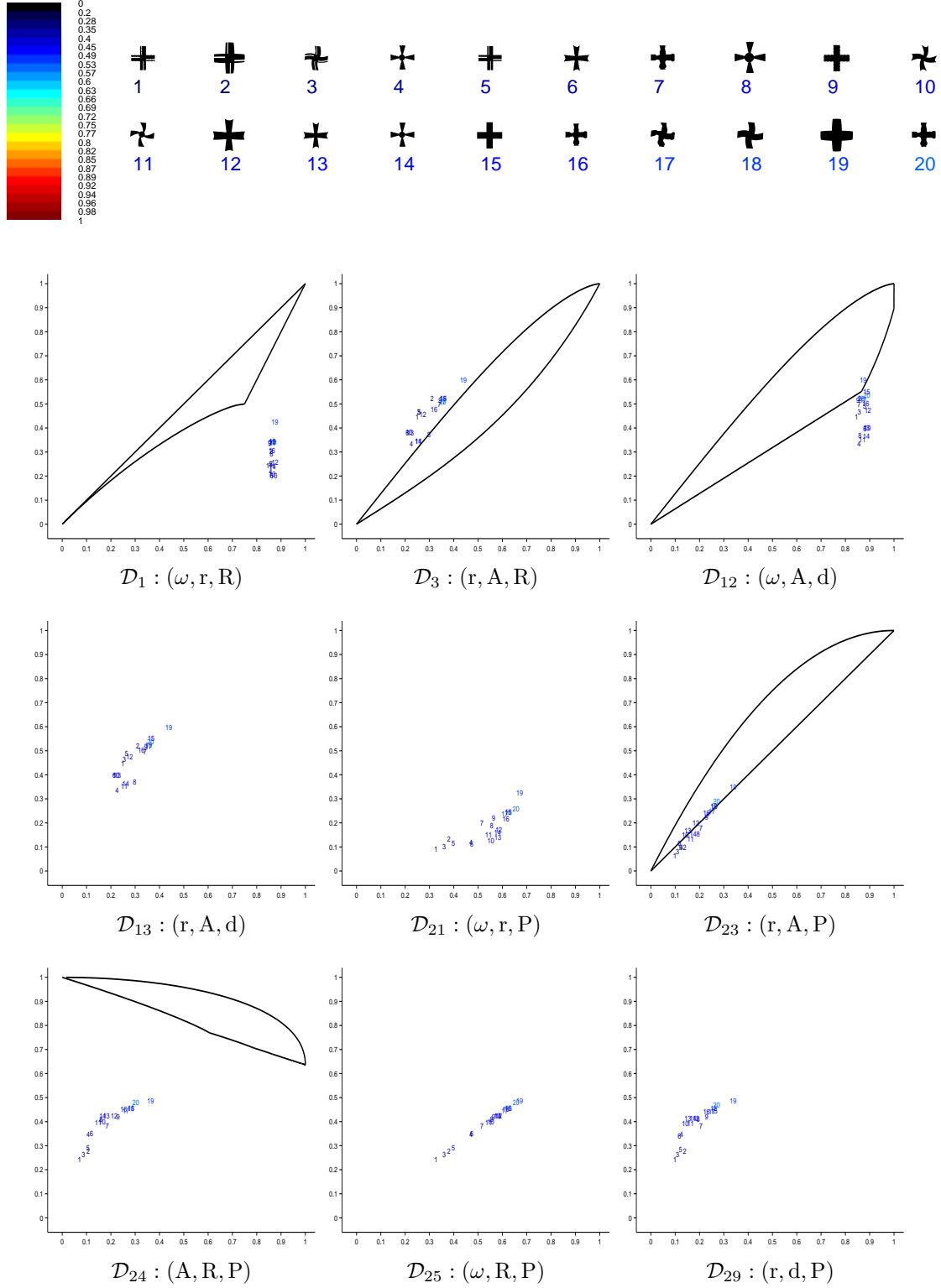


Figure 6.3: Family \mathcal{F}_5^{dsc} of twenty 2D discretized simply connected compact sets with 'cross' shape, mapped into nine shape diagrams (chosen according to the results synthetized in [9]). The color of the number is related to the convexity parameter value.

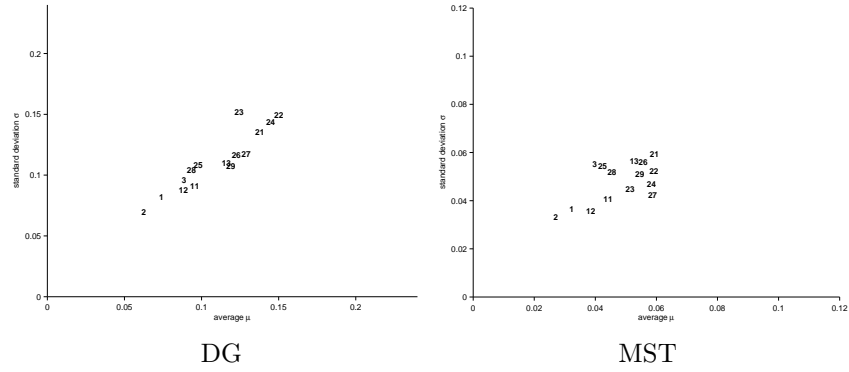


Figure 6.4: Two dispersion quantifications for all shape diagrams applied on the family \mathcal{F}_3^{dsc} . For each representation (according to the models DG and MST, respectively), indices $k \in \llbracket 1, 29 \rrbracket \setminus (\llbracket 4, 10 \rrbracket \cup \llbracket 14, 20 \rrbracket)$ of the shape diagrams \mathcal{D}_k is located according to its μ and σ values.

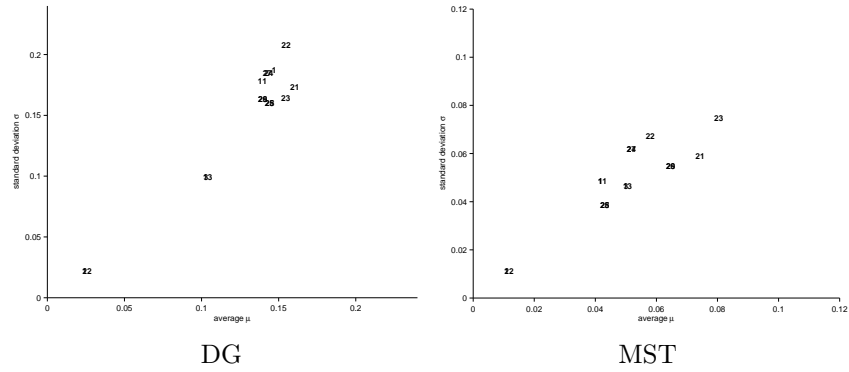


Figure 6.5: Two dispersion quantifications for all shape diagrams applied on the family \mathcal{F}_4^{dsc} . For each representation (according to the models DG and MST, respectively), indices $k \in \llbracket 1, 29 \rrbracket \setminus (\llbracket 4, 10 \rrbracket \cup \llbracket 14, 20 \rrbracket)$ of the shape diagrams \mathcal{D}_k is located according to its μ and σ values.

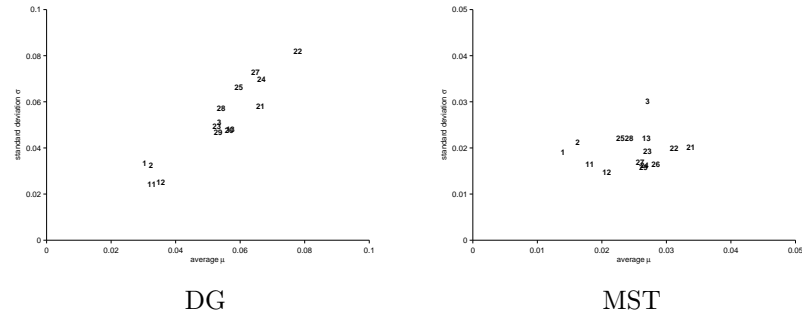


Figure 6.6: Two dispersion quantifications for all shape diagrams applied on the family \mathcal{F}_5^{dsc} . For each representation (according to the models DG and MST, respectively), indices $k \in \llbracket 1, 29 \rrbracket \setminus (\llbracket 4, 10 \rrbracket \cup \llbracket 14, 20 \rrbracket)$ of the shape diagrams \mathcal{D}_k is located according to its μ and σ values.

The results obtained allows to reveal that the shape diagrams \mathcal{D}_2 and \mathcal{D}_{12} do not discriminate the sets in each family \mathcal{F}_3^{dsc} , \mathcal{F}_4^{dsc} and \mathcal{F}_5^{dsc} . This discrimination appears little stronger for the shape diagrams \mathcal{D}_1 and \mathcal{D}_{11} . From a global vision, the shape diagrams \mathcal{D}_{21} and \mathcal{D}_{22} strongest discriminate these sets.

7 SYNTHESIS

To obtain a strong discrimination of 2D discretized simply connected compact sets, it is necessary to have both a strong dispersion and a strong convexity discrimination.

- The shape diagram \mathcal{D}_4 , \mathcal{D}_5 , \mathcal{D}_6 , \mathcal{D}_{14} , \mathcal{D}_{15} and \mathcal{D}_{16} are excluded due to their weak dispersion and convexity discrimination results.
- The shape diagram \mathcal{D}_{30} presents a strong convexity discrimination although its weak dispersion result.
- The dispersion quantification of the shape diagrams \mathcal{D}_1 , \mathcal{D}_2 , \mathcal{D}_3 , \mathcal{D}_{11} , \mathcal{D}_{12} , \mathcal{D}_{13} , \mathcal{D}_{21} , \mathcal{D}_{22} , \mathcal{D}_{23} , \mathcal{D}_{24} , \mathcal{D}_{25} , \mathcal{D}_{26} , \mathcal{D}_{27} , \mathcal{D}_{28} and \mathcal{D}_{29} gives strong values.
- The convexity discrimination is stronger for \mathcal{D}_{24} , \mathcal{D}_{25} , \mathcal{D}_{26} , \mathcal{D}_{27} , \mathcal{D}_{28} and \mathcal{D}_{29} .
- The similar sets discrimination appears stronger for \mathcal{D}_{21} and \mathcal{D}_{22} .

Futhermore, among the shape diagrams \mathcal{D}_{24} , \mathcal{D}_{25} , \mathcal{D}_{26} , \mathcal{D}_{27} , \mathcal{D}_{28} and \mathcal{D}_{29} that obtain the best results for dispersion quantification and convexity discrimination, only \mathcal{D}_{24} , \mathcal{D}_{26} and \mathcal{D}_{28} are based on known complete systems of inequalities. Observing in details the representation of quantifications for these three shape diagrams, \mathcal{D}_{24} retained for shape discrimination of analytic simply connected compact sets, is also retained for shape discrimination of discretized simply connected compact sets.

This analysis is summarized in Table 7.1.

	Complete system of inequalities	Non-complete system of inequalities
Strong discrimination	$\boxed{\mathcal{D}_{24}}$, \mathcal{D}_{26} , \mathcal{D}_{28}	$\boxed{\mathcal{D}_{25}}$, \mathcal{D}_{27} , \mathcal{D}_{29}
Moderate discrimination	$\boxed{\mathcal{D}_1}$, $\boxed{\mathcal{D}_3}$, \mathcal{D}_{11} , $\boxed{\mathcal{D}_{12}}$, \mathcal{D}_{22} , $\boxed{\mathcal{D}_{23}}$	\mathcal{D}_2 , $\boxed{\mathcal{D}_{13}}$, $\boxed{\mathcal{D}_{21}}$
Weak discrimination	$\boxed{\mathcal{D}_4}$, \mathcal{D}_5 , \mathcal{D}_6 , \mathcal{D}_{14} , $\boxed{\mathcal{D}_{15}}$, \mathcal{D}_{16} , $\boxed{\mathcal{D}_{30}}$	

Table 7.1: Shape diagrams classification according to their quality of shape discrimination of discretized simply connected compact sets and according to the completeness of associated systems of inequalities.

8 GLOBAL SYNTHESIS FOR THE THREE PARTS OF THIS STUDY

For each part of this study [8, 9], the synthesis gives the shape diagrams that provide the strongest shape discrimination. These are \mathcal{D}_{12} and \mathcal{D}_{24} . Table 9.1 gathers the syntheses.

9 CONCLUSION

This paper has dealt with shape diagrams of 2D non-empty analytic and discretized simply connected compact sets built from six geometrical functionals: the area, the perimeter, the radii of the inscribed and circumscribed circles, and the minimum and maximum Feret diameters. Each set is represented by a point within a shape diagram whose coordinates are morphometrical functionals defined as normalized ratios of geometrical functionals. From existing morphometrical functionals for these sets, twenty-two shape diagrams can be built. A detailed comparative study has been performed in order to analyze the representation relevance and discrimination power of these shape diagrams. It is based on the dispersion quantification and convexity discrimination from compact set locations in diagrams. Among all the shape diagrams, six present a strong convexity discrimination of sets, three are based on complete system of inequalities. Among these three diagrams, the shape diagram $\mathcal{D}_{24} : (A, R, P)$ is retained for its representation relevance and discrimination power.

The purpose of this paper was to present the third part of a general comparative study of shape diagrams. The focus was placed on convexity discrimination of analytic and discretized simply connected compact sets. The two first parts [8, 9] was restricted to the analytic compact convex and simply connected compact sets, respectively. For an analytic set, the geometrical functionals were accurately calculated. For a discretized set, they are estimated. Thus, in the discrete case, the shape diagrams are based on estimated morphometrical functionals.

Actually, the authors work on the case of hollowed sets (analytic and discretized) which is not specifically considered in this paper.

	Complete system of inequalities			Non-complete system of inequalities		
	Analytic compact convex sets [8]	Analytic simply connec- ted compact sets [9]	Convexity discrimination	Analytic compact convex sets [8]	Analytic simply connec- ted compact sets [9]	Convexity discrimination
Strong discrimination	$\mathcal{D}_3, \mathcal{D}_{12}, \mathcal{D}_{22}, \mathcal{D}_{23}$	$\mathcal{D}_3, \mathcal{D}_{22}, \mathcal{D}_{23}, \mathcal{D}_{24}, \mathcal{D}_{26}$	$\mathcal{D}_{24}, \mathcal{D}_{26}, \mathcal{D}_{28}$	$\mathcal{D}_2, \mathcal{D}_{13}$	$\mathcal{D}_{13}, \mathcal{D}_{21}, \mathcal{D}_{27}, \mathcal{D}_{29}$	$\mathcal{D}_{25}, \mathcal{D}_{27}, \mathcal{D}_{29}$
Moderate discrimination	$\mathcal{D}_1, \mathcal{D}_7, \mathcal{D}_9, \mathcal{D}_{11}, \mathcal{D}_{18}, \mathcal{D}_{24}, \mathcal{D}_{26}, \mathcal{D}_{28}$	$\mathcal{D}_1, \mathcal{D}_{11}, \mathcal{D}_{12}, \mathcal{D}_{28}$	$\mathcal{D}_1, \mathcal{D}_3, \mathcal{D}_{11}, \mathcal{D}_{12}, \mathcal{D}_{22}, \mathcal{D}_{23}$	$\mathcal{D}_8, \mathcal{D}_{17}, \mathcal{D}_{19}, \mathcal{D}_{21}, \mathcal{D}_{25}, \mathcal{D}_{27}, \mathcal{D}_{29}$	$\mathcal{D}_2, \mathcal{D}_{25}$	$\mathcal{D}_2, \mathcal{D}_{13}, \mathcal{D}_{21}$
Weak discrimination	$\mathcal{D}_4, \mathcal{D}_5, \mathcal{D}_6, \mathcal{D}_{10}, \mathcal{D}_{14}, \mathcal{D}_{15}, \mathcal{D}_{16}, \mathcal{D}_{20}, \mathcal{D}_{30}$	$\mathcal{D}_4, \mathcal{D}_5, \mathcal{D}_6, \mathcal{D}_{14}, \mathcal{D}_{15}, \mathcal{D}_{16}, \mathcal{D}_{30}$	$\mathcal{D}_4, \mathcal{D}_5, \mathcal{D}_6, \mathcal{D}_{14}, \mathcal{D}_{15}, \mathcal{D}_{16}, \mathcal{D}_{30}$	\mathcal{D}_{31}		

Table 9.1: Shape diagrams classification according to their quality of shape discrimination and according to the completeness of associated systems of inequalities.

REFERENCES

- [1] J.D. Boissonnat and M. Yvinec. *Algorithmic geometry*. Cambridge University Press (1998).
- [2] A. Cauchy. *Notes sur divers théorèmes relatifs à la rectification des courbes, et à la quadrature des surfaces*. Comptes-rendus à l'Académie des Sciences de Paris. **13**: 1060-1063 (1841). Oeuvres complètes, Gauthier-Villars, Paris, **6**: 369-375 (1888).
- [3] M.W. Crofton. On the theory of local probability, applied to straight lines drawn at random in a plane. *Philosophical Transactions of the Royal Society of London*. **158**: 181-199 (1868).
- [4] L.R. Feret. La grosseur des grains des matières pulvérulentes. *Premières Communications de la Nouvelle Association Internationale pour l'Essai des Matériaux. Groupe D*: 428-436 Zürich (1930).
- [5] R. Klette and A. Rosenfeld. *Digital Geometry: Geometric Methods for Digital Picture Analysis*. Morgan Kaufmann Publishers Inc. San Francisco, CA, USA (2004).
- [6] H. Poincaré. *Calcul des Probabilités*. (1896). Paris 1912, reprinted 1923.
- [7] B.N. Raby, M. Polette, C. Gilles, C. Clavel, K. Strumane, M. Matos, J.M. Zahm, F. Van Roy, N. Bonnet and P. Birembaut. Quantitative cell dispersion analysis: new test to measure tumor cell aggressiveness. *International Union Against Cancer*. **93**: 644-652 (2001).
- [8] S. Rivollier, J. Debayle and J.C. Pinoli. Shape diagrams for 2D compact sets - Part I: analytic convex sets. *Australian Journal of Mathematical Analysis and Applications*. **7(2-3)**: 1-27 (2010).
- [9] S. Rivollier, J. Debayle and J.C. Pinoli. Shape diagrams for 2D compact sets - Part II: analytic simply connected sets. *Australian Journal of Mathematical Analysis and Applications*. **7(2-4)**: 1-21 (2010).
- [10] L.A. Santaló. Sobre los sistemas completos de desigualdades entre tres elementos de una figura convexa plana. *Math. Notae*. **17**: 82-104 (1961).
- [11] D. Sharvit, J. Chan, H. Tek and B.B. Kimia. Symmetry-based indexing of image databases. *Visual Communication and Image Representation*. **9**: 366-380 (1998).
- [12] J. Zunic and P.L. Rosin. A new convexity measure for polygons. *IEEE Transactions on Pattern Analysis and Machine Intelligence*. **26**: (7) 923-934 (2004).

ECOLE NATIONALE SUPÉRIEURE DES MINES DE SAINT-ETIENNE, CIS - LPMG, UMR CNRS 5148, 158 COURS FAURIEL, 42023 SAINT-ETIENNE CEDEX 2, FRANCE, TEL.: +33-477-420219 / FAX: +33-477-499694,

E-mail address: rivollier@emse.fr ; debayle@emse.fr ; pinoli@emse.fr